Biomass Conversion and Biorefinery
https://doi.org/10.1007/s13399-022-03593-9

ORIGINAL ARTICLE

Investigating solids present in the aqueous stream during STEX condensate upgrading—a case study

Dag Helge Hermundsgård[1,2] · Solmaz Ghoreishi[1] · Mihaela Tanase-Opedal[3] · Rune Brusletto[2] · Tanja Barth[1]

Received: 23 August 2022 / Revised: 16 November 2022 / Accepted: 23 November 2022

Abstract
Steam explosion (STEX) of woody biomass is an efficient pretreatment method in the production of water-resistant wood pellets. The STEX process also generates an aqueous condensate stream containing dissolved organic compounds, with furfural as the most abundant and valuable component. An industrial-scale recovery process for furfural and other organic by-products is therefore in the process of being developed and built. One challenge in the process has turned out to be the formation of solid particulate matter that can clog filters in the process unit. We have analyzed both the solid deposits and the fluids present at different points in the process unit to try to identify the origin of the particles using spectroscopic and chromatographic analysis, elemental analysis, and scanning electron microscopy.
The aqueous fluids deriving from condensed steam contain furfural and other small organic molecules, with a separate low-density organic layer occurring at some points. This layer largely consists of wood extractives, typically terpenoids. In addition, a heavy organic phase comprising mostly furfural was found at one sampling point. The particles comprise a black, largely insoluble material with a H/C ratio of 0.88 and an O/C ratio of 0.26 and a very low ash content. IR spectra show a low content of C–H functional groups, and chromatographic analysis supports an interpretation that the particles are dominantly furfural-sourced humin-like polymers with adsorbed or co-polymerized terpenoids. Particle formation has been reproduced in a laboratory setting with conditions similar to those in the full-scale process.

Keywords Biorefinery · Steam explosion · Condensate · Furfural · Terpenoids

1 Introduction

Increasing the use of renewable carbon-based resources requires the development of efficient biorefinery options to maximize the utilization of biomass feedstocks. In this context, a biorefinery for producing resilient black pellets and bio-based chemicals from wood as feedstocks has been established in Norway [1]. The concept comprises steam explosion (STEX) of sawdust for pellets production and recovery of bio-based chemicals from the condensed steam and wet steam-exploded mass. Furfural is the most important product found in the condensed steam, and there is also an option for recovering 5-hydroxymethylfurfural (HMF) and sugars by washing and pressing the steam-exploded mass [2].

Establishing a novel, full-scale, efficient production plant is a challenge, and unexpected by-products can appear. In this case, the operation of the refinery unit for recovering furfural has been hampered by the formation of solid black particles that cause clogging of filters in the process flow, impeding the production rate of furfural and slowing down the water treatment. This reduces the production capacity of the refinery, as these are essential processes; hence, understanding the origin and formation pathway for the particles is crucial for developing suitable strategies for prevention.

The condensed steam from the STEX reactor contains the volatile fractions of extractives, such as terpenoids, and the reaction products from labile biomass polymers, especially those from hemicellulose. The feedstock also contains other extractives, such as fatty acids and resin acids that follow the steam-exploded biomass. Extractives are well

✉ Dag Helge Hermundsgård
Dag.Hermundsgard@uib.no

[1] Department of Chemistry, University of Bergen, Norway, Allégaten 41, N-5007 Bergen, Norway

[2] Arbaflame AS, Henrik Ibsens gate 90, N-0230 Oslo, Norway

[3] RISE PFI AS, Høgskoleringen 6B, NO-7491 Trondheim, Norway

Published online: 03 December 2022

described in literature on the composition of wood, see, e.g., Fig. 1 [3], and the terpenoids comprise a large part of this compound class. They include hydrocarbon species and oxygen-containing structures with carbonyl, ether, and hydroxyl compounds, often with cyclic structures and some degree of unsaturation.

The products from the thermal breakdown of hemicellulose (Fig. 2) are also a source of reactive molecules in the system. The furanic structures are prominent, like furfural and HMF, together with smaller molecules like methanol, acetic and formic acid, and acetone. Both the furans and the terpenoids can participate in polymerization reactions that can ultimately lead to black precipitates and are thus candidates as a source for the observed solid particles. One class of such particles, often termed *humins*, are solid condensation products which occur by random polymerization processes during acid-catalyzed dehydration of sugars [4]. Both pentose and hexose sugars, as well as furans like HMF, have been reported to contribute to the formation of humins, and although their formation routes and molecular structure are not fully established, research strongly suggests that humins from different sources will have differences in structure [5–7]. Formation of solid by-products like humins is a constant challenge in industrial processes, where they impede production and reduce operational efficiency, which leads to negative effects on the economics of the production process. Looking at results from the acid-catalyzed conversion of different sugar molecules to levulinic acid seems to suggest that humin formation cannot be prevented and a better understanding of their formation and how to handle them is therefore the key to reducing their undesirable effects [8–11].

In this work, black particles recovered from a filter in a side-stream processing unit for condensed steam at the ArbaOne plant have been analyzed in terms of composition and solubility, using a wide range of spectroscopic and chromatographic analytical procedures. The analytical results are evaluated in terms of suggesting a pathway for the formation of the particles from the organic components available in the condensate stream. Laboratory-scale experiments to replicate the formation of black particles have also been performed.

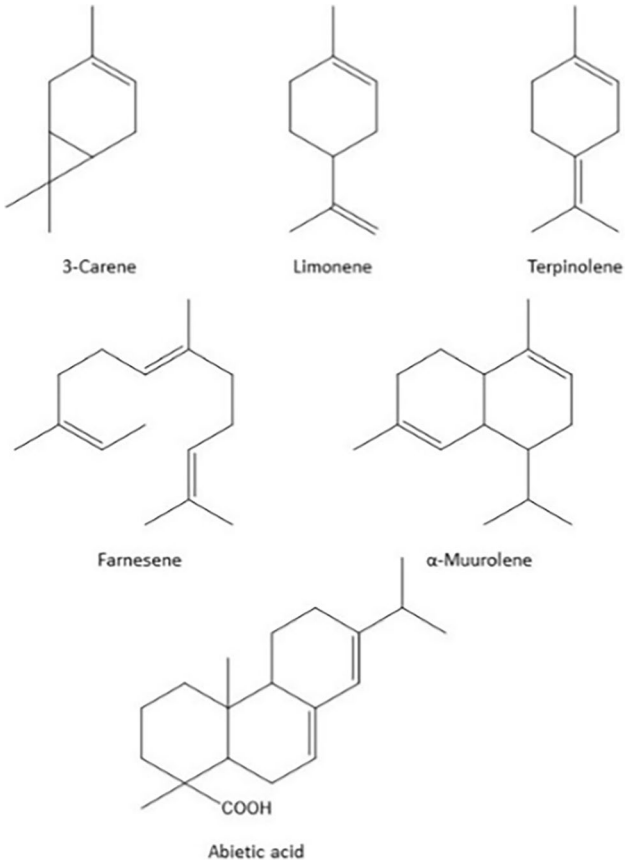

Fig. 1 Examples of terpenoids found in wood extractives (adapted from Sjöström [3])

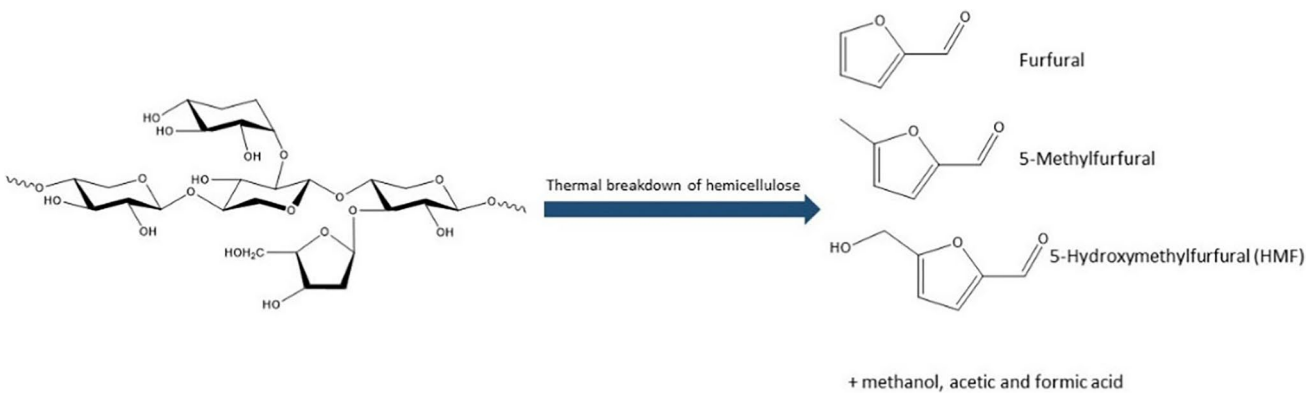

Fig. 2 Furanic compounds produced from STEX of woody biomass

2 Materials and methods

All reagents and solvents were purchased from Merck KGaA (Darmstadt, Germany) and used without any further purification. All standard components are commercially available.

2.1 The steam explosion process

The steam explosion pretreatment was performed at the ArbaOne pelleting plant, operated by Arbaflame AS, located in the south-eastern part of Norway. A feedstock consisting of sawdust from a mixture of spruce and pine, both softwoods, in an unknown, variable ratio is treated with saturated steam in a large-scale 11.5-m^3 reactor with pressures of 19–23 bar and a reaction time of 500 s. Reaction temperatures reach between 212 and 222 °C during cooking, which is optimal for the production of water-resistant pellets. However, this temperature is also ideal for the formation of furanic compounds. These reaction conditions comprise a severity [12] of about 4.22 for the case of 212 °C up to 4.51 when the temperature reaches 222 °C.

During the decompression, high-pressure steam is released from the reactor and subsequently cooled in condensers and collected in the demister tank (Fig. 3). From the demister, the acidic condensate (pH 2.5–3) flows through a skimmer tank, where a significant part of the extractives are removed from the liquid. The condensate is then fed through an ultra-filtration unit (UF), removing particles larger than 0.05 µm, to a temporary storage tank that feeds condensate through a distillation tower to separate furfural and low boilers from the aqueous condensate, as illustrated in Fig. 3.

The main components and typical concentrations of the condensate are as follows: furfural, 18.1 g/L; 2-acetylfuran, 0.2 g/L; 5-methyl furfural, 0.4 g/L; HMF, 0.4 g/L; acetic acid, 9.3 g/L; formic acid, 1.9 g/L; methanol, 5.5 g/L; and a small, but un-quantified, amount of residual sugars.

The distillation unit separates low boilers and furfural from the condensate in a continuous two-step process. The first column operates at 1100 mbar and in the range of 70–105 °C, where low boilers are removed from the condensate, and the second column operates at 150 mbar and between 50 and 56 °C and removes the furanic compounds, mainly furfural, from the condensate stream before the stripped condensate can be sent to the water treatment plant. While the black particles were first found in a strainer after the first column, a closer investigation uncovered that the actual earliest source of the black particles in the process stream is a heat exchanger that heats the condensate to a temperature of about 96–104 °C, before it enters the first column.

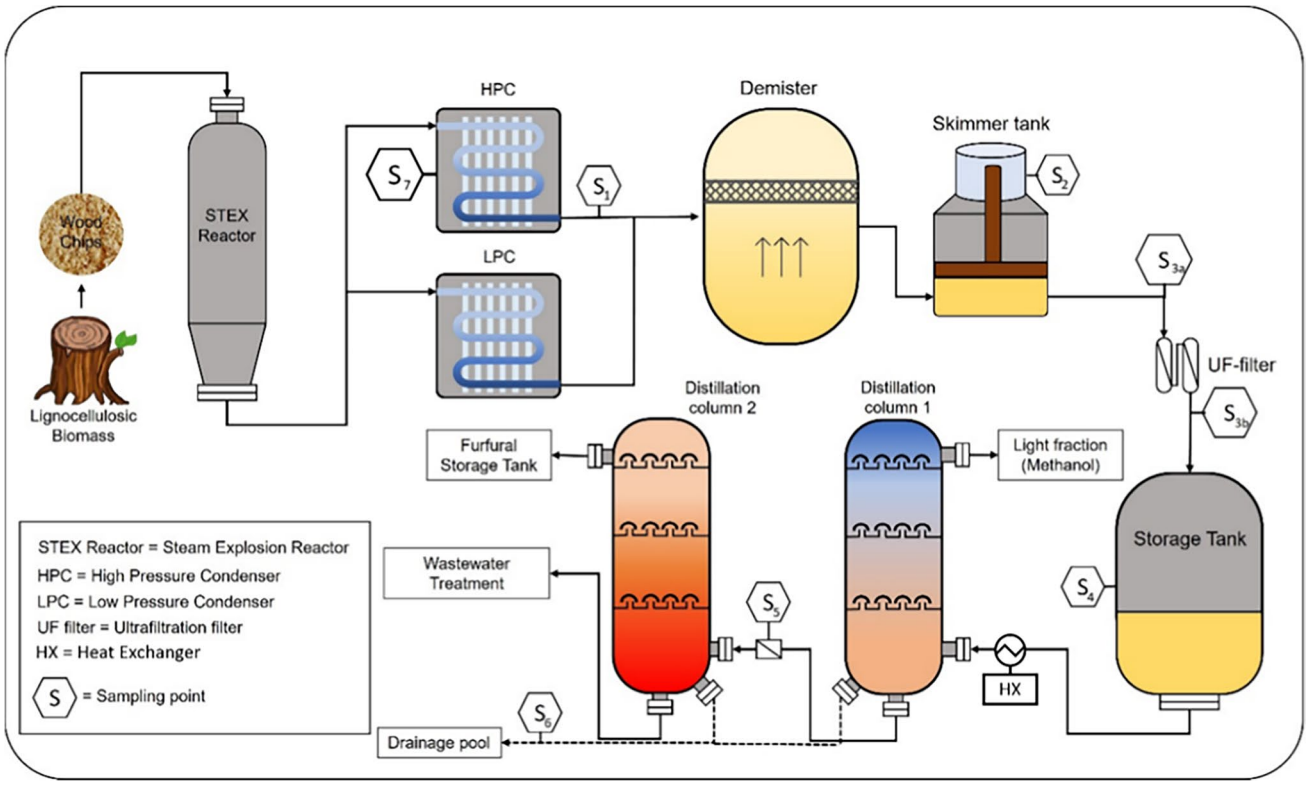

Fig. 3 Overview of ArbaOne process flow with sampling locations marked ([13, 14] recreated by Joakim L. Molnes)

2.2 Sampling

In order to get a better understanding of where the black particles originate, samples taken from several points in the process chain were analyzed. Figure 3 shows a simplified flowchart of ArbaOne's process chain, with markers showing the sampling points along the process chain. The sample information is given in Table 1.

2.3 Analysis of the black particles

2.3.1 FT-IR of black particles

A sample of the black particles (sample #5, Table 1) was crushed into a rough powder before being applied to an attenuated total reflectance (ATR) crystal, where a spectrum was acquired (Fig. 5).

2.3.2 Elemental analysis

Elemental analysis was performed on a sample of the black particles (sample #5, Table 1), and a van Krevelen diagram (Fig. 12) was created to compare the elemental composition of the black particles to that of relevant carbohydrates from lignocellulose, furans, and furfural-derived humins.

2.3.3 SEM

A sample of roughly crushed black particles (sample #5, Table 1) was coated with a thin layer of 60% palladium and 40% gold before being placed in a Fei Quanta 450 scanning electron microscope where pictures of the surface structure were taken (Fig. 6).

2.3.4 Ash content

The ash content of the black particles (sample #5, Table 1) was quantified with two parallels at 525 °C and 900 °C according to ISO 1762 and ISO 2144, respectively.

2.3.5 ICP-MS

A sample of 0.24 g of black particles (sample #5, Table 1) was dissolved into a homogeneous solution with 10 mL of concentrated nitric acid. Before analysis, the sample was diluted with 2% w/v HNO_3 to a dilution factor of 825. The sample of black particles was then analyzed for trace amounts of a range of elements (Al, Cr, Mn, Fe, Ni), with a Thermo Scientific Element XR high-resolution inductively coupled plasma mass spectrometer.

Table 1 Overview of samples taken from the process line and what analysis was performed on the different samples. The sampling points are marked in the process sketch in Fig. 3

Sample #	Sample type (phase)	Location	Analysis	Additional notes
1	Condensate (liquid)	Condensate from the HPC outlet	FT-IR and GC–MS of the organic top layer	Analysis after fractionation
2	Skimmer tank product (organic liquid/solid particles)	Skimmer tank product container	NMR/IR	Product from the skimmer tank
3a	Condensate (liquid)	Before UF	Visually inspected (filtration)	No black particles were found
3b	Condensate (liquid)	After UF	Visually inspected (filtration)	No black particles were found
4	Brown particles (solid/semi-solid)	Storage tank	Particles were found, not enough for systematic analysis	Some brown particles were found when the tank was drained and inspected
5	Black particles (solid)	Filter before the inlet to column 2	Ash content, FT-IR, ICP-MS, SEM, GC–MS, Pyr-GC–MS, TGA-FTIR	The black particles were collected from the filter and analyzed in the state they were found
6	Black organic liquid (organic liquid)	Distillation unit drainage pipes	NMR, FT-IR	Black organic liquid found together with water/condensate
7	Black solid residue	HPC	FT-IR, TGA-FTIR, Pyr-GC–MS	Residue found during maintenance, somewhat resembling the black particles
8	Black solids	Laboratory	FT-IR	Solid material collected after laboratory experiments at various conditions

2.3.6 Pyrolysis GC–MS

Organic compounds in the samples were also characterized using pyrolysis GC–MS (pyrolysis gas chromatography-mass spectroscopy). Samples of 3–5 mg (sample #5 and #7, Table 1) were pyrolyzed at 600 °C in a reactor from Frontier Lab (3050TR).

2.3.7 TGA-FTIR

Thermogravimetric analysis was conducted on a NETZSCH STA 449F3 Jupiter instrument. Samples of 10 (± 1) mg (sample #5 and #7, Table 1) were individually heated in an inert atmosphere of N_2.

The evolved gasses from the TGA analyzer then entered a PerkinElmer Spectrum 3 FT-IR where an absorbance spectrum and a 3D surface plot were collected (Figure S5 and S6 in the supplementary file).

2.3.8 Solubility of black particles and Soxhlet extraction for GC–MS analysis

To perform a GC–MS analysis of the particles, an attempt was made to dissolve a small sample of particles in one of the three common solvents, acetone, ethyl acetate, and tetrahydrofuran (THF). The samples were stirred overnight (about 14 h), and though none of the solvents was able to fully dissolve all the material, THF was by visual inspection determined to be the best solvent (Figure S1 in supplementary material), and a Soxhlet extraction was performed.

When performing the extraction, 1.5 g of the black particles (sample #5, Table 1) was extracted with THF for 20 h using Soxhlet extraction. For analysis with GC–MS, 1 mL of the solution from the Soxhlet extraction was diluted with 10 mL THF.

In order to more thoroughly evaluate the solubility of the black particles (sample #5, Table 1), a range of common and less common solvents with different polarities were tested by weighing and adding a sample of black particles to the solvent and stirring for 24 h. The samples were then filtered with a 1.6-µm pore size glass fiber filter, before the particles were weighed again and the dissolved mass calculated. Results from the solubility tests can be found in Table S3 in the supplementary file. It is important to note that the expanded solubility test has been done with a different batch of black particles than the rest of the experiments, due to a shortage of material from the initial batch. The visual difference between the batches can be seen in Figures S1 and S2 in the supplementary file.

Similarly, the solubility of the black residue from the HPC (sample #7, Table 1) was assessed, and it was shown to be far more soluble in ethyl acetate than the black particles from the distillation unit, although it was not completely dissolved.

2.4 Analysis of other organic liquids and samples

2.4.1 FT-IR of organic samples

Samples of liquid organics from condensates (sample #1, Table 1), the skimmer tank (sample #2, Table 1), and the drainage pipes (sample #6, Table 1) were applied in small amounts to the ATR crystal with a glass pipette and an IR spectrum was acquired (Figs. 7 and S7 respectively).

2.4.2 Sample preparation and acquisition of qNMR spectra for NMR analysis

A portion of the black organic liquid (sample #6, Table 1) was prepared for qNMR analysis. Using 0.56 g of the organic liquid and adding 1.92 mL of deuterated chloroform (CDCl3, containing 0.03% TSP (3-(trimethylsilyl)-propionic-2,2,3,3-d_4 acid)). Finally, 600 µL of the prepared sample was then transferred to a 5.0 × 103.5 mm Sample-jet NMR tube with an Eppendorf autopipette.

2.4.3 Fractionation of condensates

A condensate sample (sample #1, Table 1) of approximately 200 g was placed into a round-bottom flask and fractionated into 4 fractions using a rotary evaporator at 50 °C with decreasing pressure from 90 to 60 mbar. From the remaining non-volatile fraction, 0.1 g was dissolved in 9 mL EtOAc, with 1 µL/L (IS) and analyzed by GC–MS.

2.5 Instrumental conditions

2.5.1 FT-IR instrumental conditions

The FT-IR spectra of the black particles and organic liquids from the condensate stream were acquired on a Thermo Fisher Nicolet iS5 instrument with an attenuated total reflectance (ATR) crystal. The main measurement features were a spectral range from 4000 to 400 cm^{-1}, 16 scans, and a resolution of 4 cm^{-1}.

2.5.2 Elemental analysis instrumental conditions

Elemental analysis was performed in CHNS mode with a VarioEL III from Elementar, using helium as carrier gas and calculating the oxygen amount by difference.

2.5.3 Instrumental conditions for the acquisition of NMR spectra

^{1}H NMR analysis of the sample was performed on a 600-MHz Bruker AVANCE NEO NMR-spectrometer equipped with a QCI-P CryoProbe at 298 K. The pulse sequence applied was zg0 using a 90° ^{1}H pulse with a spectral width of 28 ppm, 128 k data points, 8 scans, and 0 dummy scans. The relaxation delay was set to 60 s to ensure complete relaxation between scans. The spectrum was zero-filled to 256 k data points and processed using a line broadening of 0.3 Hz.

2.5.4 SEM instrumental conditions

The Fei Quanta 450 scanning electron microscope is using a thermal field emission filament and has a range of 200 V–30 kV with a resolution of 0.8 nm at 30 kV for up to 1,000,000 × magnification. The microscope uses variable pressure and is fitted with a secondary electron detector and a backscatter detector.

2.5.5 ICP-MS instrumental conditions

Quantification of the sample is done with the use of external calibration curves (multi-element standard solutions prepared from certified single-element solutions from Spectrapure) and indium is used for internal standardization.

No relevant reference material was available, so as a direct control of the calibration curves and to monitor the performance during the analytical runs, certified reference material in the form of synthetic water, SPS-SW-2 from Spectrapure Standards AS, is analyzed repeatedly throughout the run.

2.5.6 Pyr-GC–MS instrumental conditions

The pyrolytic compounds were separated in the GC (7890B) using an Ultra ALLOY-1 capillary column (30 m–0.25 mm id, 2.0-µm film) and identified using MS (5977B MSD), both from Agilent Technologies.

2.5.7 TGA-FTIR instrumental conditions

For each sample, using dynamic thermogravimetry, the TGA was triggered between 35 and 900 °C, in the inert N_2 atmosphere. The purge nitrogen flowrate was set to 40 mL/min and the protective nitrogen flow to 60 mL/min.

With FT-IR, the evolved gasses from TGA were analyzed, with both an absorbance spectrum and a 3D surface plot collected in the 530–4000-cm^{-1} wavenumber range, with 32 scans per specimen.

2.5.8 GC–MS instrumental conditions

All samples prepared for GC–MS were analyzed on an Agilent Technologies 7890A GC system with an autosampler coupled with an Agilent 5977A mass-selective detector (MSD). The injection was run in splitless mode, with an injector temperature of 280 °C. A 30-m HP-5 ms column with 250 µm i.d. and thickness of 0.25 µm from Agilent Technologies was used. The following GC–MS instrumental conditions were applied: start temperature: 40 °C (held for 5 min), heating rate 1: 6 °C min^{-1} to 280 °C, and heating rate 2: 40 °C min^{-1} to 300 °C (held for 5 min). The GC–MS interphase valve delay was set to 4.60 min and the MS detector was operated in the positive mode at 70 eV with an ion-source temperature of 250 °C. Compounds were identified using Enhanced MSD Chemstation software F.01.00.1903 and the NIST 2.0 library.

2.6 Preparation of reference samples

2.6.1 Reflux cooking of condensates

To replicate the formation of the black particles in a laboratory environment, several experiments were conducted with a total reflux system as to simulate conditions similar to the distillation unit at ArbaOne. Condensate samples (sample #1, Table 1) were heated under stirring in an attempt to generate solid humins for comparison with the black particles (sample #5, Table 1), in an experimental setup consisting of a round flask, submerged into an oil bath for heating, and a water-cooled spiral cooler attached to the flask.

For each experiment, a sample of condensate (sample #1, Table 1) of 75 mL was added to the round flask, heated to boiling, and held at boiling temperature for about 72 h.

2.6.2 Seeding with black particles and added furfural

To investigate what may cause further growth of the black particles, a sample of black particles (sample #5, Table 1), collected from the Arbaflame plant, was added to a condensate sample to work as seeding particles and boiled with the condensates as described in Sect. 2.6.1. In parallel, another 75 mL of the condensate sample with seeding particles was prepared, but in addition to a sample of seeding particles, 4 mL of furfural (Sigma-Aldrich, 99%) was also added to the round flask before the mixture was heated and boiled. In a similar experiment, the added furfural was replaced with an addition of 0.05 g of HMF.

Two control experiments were also performed, one with distilled water and one with condensate (sample #1, Table 1).

Fig. 4 Picture of a sample of black particles found in the distillation unit (sample #5, Table 1)

Table 2 Results from the determination of ash content in the black particles show similarly low ash values at both ISO standards

Standard	Ash value [%]	Temperature [°C]	Std dev
ISO 1762	0.14	525	0.01
ISO 2144	0.14	900	0.01

Table 3 Results from ICP-MS analysis with 3 parallels of black particles show that they contain only trace amounts of inorganics

Trace elements		Al	Cr	Mn	Fe	Ni
mg/g of sample	Par 1	0.146	0.085	0.008	0.140	0.032
	Par 2	0.136	0.082	0.008	0.135	0.026
	Par 3	0.149	0.083	0.008	0.138	0.028
Average		0.144	0.083	0.008	0.138	0.027

Table 4 Estimated elemental composition of the black particles, with H/C and O/C ratios from the two parallels of the elemental analysis

	Weight%				Per carbon	
	N	C	H	O	H/C	O/C
Black particles 1	1.5E − 03	70.35	4.98	24.66	0.84	0.26
Black particles 2	8.9E − 04	70.21	5.46	24.32	0.93	0.26

A 4-mL sample of furfural (Sigma-Aldrich, 99%) was added to both before the samples were heated for 72 h. This was done to control for how much, if any, of the solid matter generated from the humin experiment could be accounted for from self-polymerization of furfural.

3 Results

3.1 Characterization of particles

A sample of the black particles (sample #5, Table 1) that was collected from a filter at the inlet of the second distillation column is shown in Fig. 4. The particles are dark black with a rough but shiny, almost metallic, surface.

3.1.1 Ash and inorganic constituents

Ash analysis at 525 °C and 900 °C provides a rough estimate of the content of inorganic material. The results given in Table 2 show that the ash content is quite low, and these results are in agreement with the ICP-MS results (Table 3).

Identification of inorganic constituents in the particles was accomplished with ICP-MS analysis, after total dissolution of a particle sample in concentrated nitric acid. The results are given in Table 3.

The ICP-MS analysis shows a variety of metallic compounds where iron (Fe), aluminum (Al), nickel (Ni), and chromium (Cr) are most prominent. With the exception of aluminum, these are metals which are commonly used in black carbon steel, found in the reactor and piping at the ArbaOne plant. The low concentration of inorganics found in the black particles shows that the particles are organic in nature and supports a theory of humin formation as their source.

3.1.2 Elemental analysis

The black particles from the distillation unit were analyzed to determine their elemental composition. The analysis was performed on the particles as received before extraction. The relationship between the carbon, oxygen, and hydrogen content that can be expected from humins is reported in the literature to be in the order of 55–65% carbon, 4–5% hydrogen, and 30–40% oxygen [10, 15–18]. The composition of the organic elements in the black particle sample (sample #5, Table 1) is shown in Table 4 and differs from the composition of humins by having a larger w% of carbon, with correspondingly lower oxygen content.

3.1.3 FT-IR spectra of the black particles

The FT-IR spectrum of the particles (sample 5, Table 1), as received, is shown in Fig. 5.

The spectra obtained from the black particle sample do not have strong absorption intensities, however finely crushed the particles were. The pattern indicates a strongly conjugated system. The lack of strong absorption bands in the C–H area is significant, indicating that saturated carbon groups are not frequent in the structure. The assignment of the major adsorption bands is given in Table S1 in the supplementary file.

3.1.4 SEM

Figure 6 shows two pictures of the surface of the black particles, taken with the scanning electron microscope at 3000 × and 10,000 × magnification, respectively. The image on the left shows both continuous areas with cracks and several noticeable spherical indentations and holes, which could indicate a porous structure. There are also areas with irregularly shaped debris and scattered spherical substances (magnified in the image on the right), resembling oily substances which could be the remains terpenoid compounds adsorbed to the surface of the black particles.

3.1.5 Pyrolysis GC–MS

Results from pyrolysis GC–MS analysis (Figure S3 in the supplementary file) showed that the volatile carbon constituents from both the black particles (sample #5, Table 1) and the dark residues (sample #7, Table 1) consist of various furanic species, phenolic groups, and terpene compounds. The data from pyrolysis GC–MS indicates that the particles

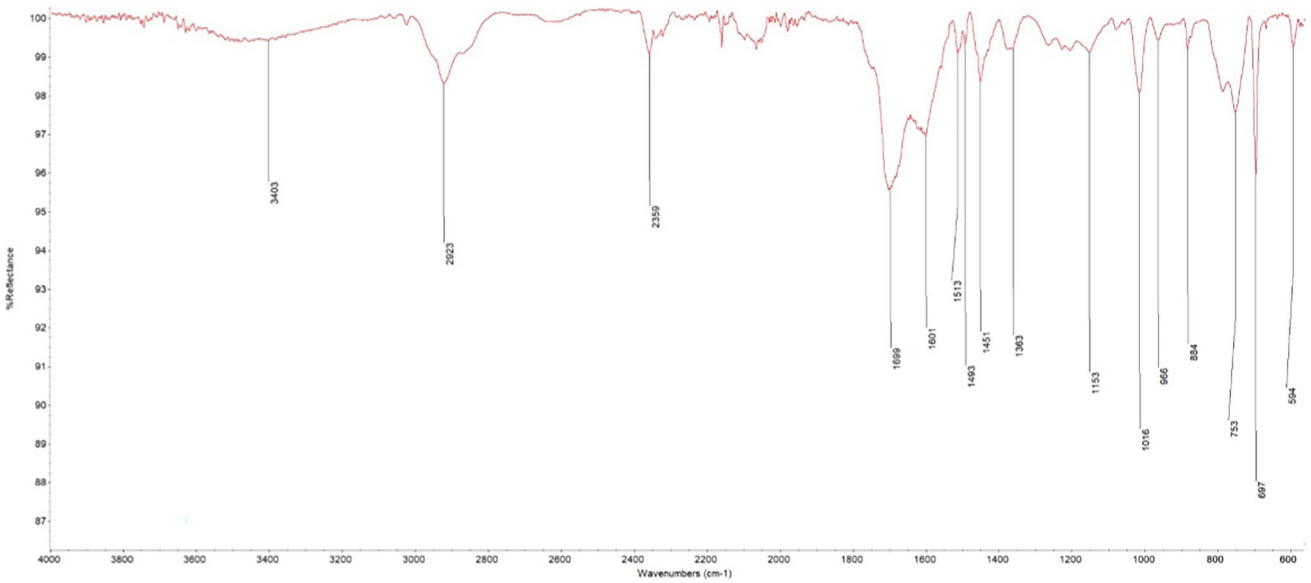

Fig. 5 IR spectrum of the black particles (sample 5, Table 1)

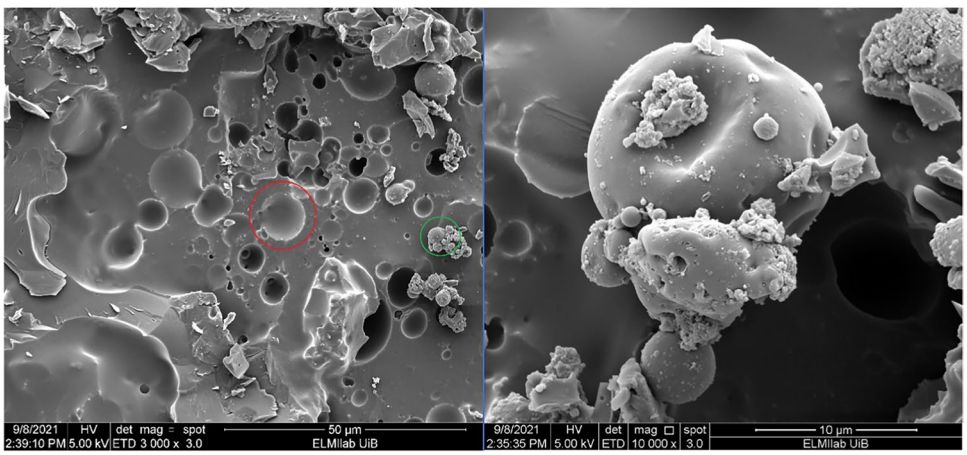

Fig. 6 Two SEM pictures. Black particles at 3000 × magnification. The red marker shows an indent on the surface and the green marker shows what may be terpenoids that have been adsorbed on the surface of the particles (L). One of the substances on the surface of the black particles at 10,000 × magnification (R)

consist of a furan-rich polymer network containing different oxygen functional groups and the results are in accordance with the literature results of van Zandvoort et al. [5] and support a hypothesis of humin formation as the source of the particles.

3.1.6 TGA-FTIR

Thermogravimetric analysis was used to study the thermal stability of the black particles, and Figure S4 in the supplementary file shows the TGA scans for both the black particles from the distillation unit (sample #5, Table 1) and from the solid dark residues found in the steam condenser (sample #7, Table 1). A mass loss of 14% from the black particles can be observed by 200 °C, which is mass loss attributed to the release of volatiles and humidity of the sample, and at the endpoint of 900 °C, a residual 20–22% of the mass remains present. In contrast to the particles, the dark residue from the condenser only shows a mass loss of 5% by 200 °C and approx. 40–43% at 900 °C, indicating a high ash content. The maximum rate of weight loss, identified by the highest intensity peak in the rate of weight change and represented by the dotted line, is found around 433 °C for both samples. The rate of mass loss for the black particles reaches approximately 5%/min at this temperature.

The high char yield for the dark particles from the reactor suggests that some condensation/polymerizations of formed fragments are possible. In addition, these results suggest that the dark residues from the HPC are very similar to what we would characterize as humins.

The evolved gasses released during TGA measurements were analyzed by FTIR. Water and CO_2 were the main gasses released during the mass loss, due to the release of volatile species. Water can be released as a by-product in condensation reactions, leading to losses in oxygenated functional groups. Because of this, CO_2 and H_2O were filtered away from the TGA-FTIR spectrum in this analysis. CH_4 was detected at 2344 cm^{-1} for the dark residues from the HPC, while in the spectrum for the dark particle from the distillation unit CH_4 can be identified at 2937 cm^{-1} (see Figures S5 and S6 in the supplementary file). In the band range from 2170 to 2000 cm^{-1}, there is the presence of gasses such as CO. The absorption peaks at 1740 cm^{-1} correspond to the vibration of carbonyl groups C = O; acetyl and carboxyl groups present in hemicelluloses and cellulose. The peaks at 1430–1602 cm^{-1} correspond to the vibration of the structure of aromatic ring (C = C) characteristic of cellulose and lignin [19].

3.1.7 Soxhlet extraction and solubility test

During the Soxhlet extraction with THF, which was determined to be the better of the solvent candidates from the initial inspection, it was only possible to dissolve 23 wt% of the black particulate matter.

The most abundant compounds from the GC–MS analysis of the extracted material are given in Table S2 and comprise mostly oxygenated terpenoids which suggest that the terpenoids may not be an important constituent in the formation of the black particles, but rather are adsorbed to the particles' surface.

The initial solubility test and Soxhlet extraction showed that the particles were not easily soluble in common solvents (Figure S1 in the supplementary file). From the expanded solubility test, acetone, ethyl acetate, and dichloromethane gave the best results, being able to dissolve 32.5–33.7 wt% of the black particles (Table S3 in the supplementary file). From the two tests, it does seem that the particles from the new batch may have a small, but still significant increase in solubility, relative to the initial test and what was achieved from Soxhlet extraction with THF. The results from the expanded solubility test still show that the solubility of the black particles is fairly limited but may also indicate that the amount of terpenoids adsorbed to the surface of the particles can vary.

Several cleaning products, meant for industrial applications, have also been tested without providing any better results. The only medium that has been able to completely dissolve the black particles so far is nitric acid, which was able to fully dissolve the black particles over a period of 24 h in a concentration as low as 20%.

For the black residues (sample 7, Table 1), further investigation of solubility was deemed not necessary, as ethyl acetate proved sufficient for dissolving the majority of the residue.

3.1.8 Calorific value

The calorific value was determined for both samples, and the results show a lower calorific value of 26 $MJkg^{-1}$ for dark residues (sample #7, Table 1) from the HPC compared to the black particles from the distillation unit (sample #5, Table 1), calorific value 32 $MJkg^{-1}$. Because of the calorific value and the TGA-FTIR results, the particles may have good fuel properties.

3.2 Characterization of other organic liquids and samples

3.2.1 Sampling

The function of the skimmer tank (sample point #2 from Fig. 3) is to remove oils, waxes, biomass residues, and resins like terpenoids from the aqueous product stream. These materials have been carried from the reactor with the condensate during the STEX decompression. From the analysis

of the skimmed organics, a major part of what is being removed here is terpenoids.

Samples of the condensate from both before and after passing the UF unit were inspected, but no black particles were found in the condensate stream. This implies that the particles either form after the filtration stage or are small enough that they can pass through the membrane and are invisible to the naked eye. Considering the pore size of the ultra-filtration unit, particle breakthrough is considered highly unlikely.

The temporary storage tank and the distillation unit are connected to enable recycling of the condensate. In such cases, the condensate could be heated and cooled several times, which could contribute to increase the polymerization reactions and by-product formation in the form of solid precipitates.

In the temporary storage tank, some similar particles with a dark brown color and oily/tar-like surface were found. As opposed to the black particles, these particles were liquidized and dissolved when heated in condensate. No further characterization was made since the sample was not large enough for further analysis.

3.2.2 FT-IR spectra

An infrared spectrum of the black organic liquid sample (sample #6, Table 1) was acquired and compared with a pure furfural sample, as shown in Figure S7. Peak assignments are given in Table S4.

The spectrum of black organic liquid found is mostly identical to that of a standard spectrum of furfural, with the exception of the small O–H stretch at 3529 cm^{-1}. This impurity likely comes from the water in the condensate, mixing with the furfural.

The non-volatile bottom fraction from the fractionated condensate sample (sample #1, Table 1) was also analyzed by FT-IR, and the spectrum is given in Fig. 7. It is different from the spectra of the black particle sample, with strong C–H signals just below 3000 cm^{-1}, indicating a terpenoid composition.

3.2.3 NMR

From the ^{1}H NMR spectrum of the black organic liquid (Fig. 8), we identify one abundant compound with 4 peaks, corresponding with proton signals we expect to find from furfural. This further supports the idea that the black liquid is a separated phase of furfural.

Several smaller signals can be seen in the spectrum, and these correspond to 2-acetylfuran, 5-methylfurfural, and some other unidentified impurities. These signals are mostly the same as those found in the furfural standard. This supports the results from the FTIR analysis in that this liquid is furfural. The dark/black color is however interesting to note. Furfural, being a colorless liquid, will darken to yellow, brown, or even black when exposed to oxygen through oxidation and condensation reactions with furfural radical intermediates [20]. The concentration of these polymerized impurities will usually not constitute more than a minor fraction of the product, even in the case of completely black furfural.

Together, the FTIR and the NMR spectra highly suggest that the black liquid indeed is furfural, which has been darkened by impurities and supports the possibility of furfural polymerization as the source of the particles.

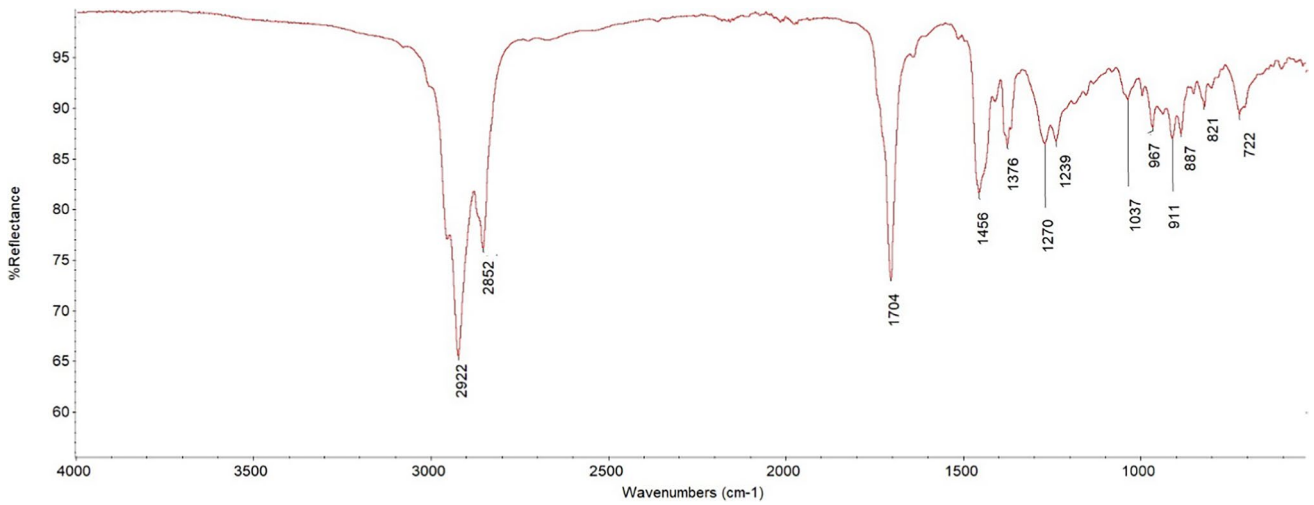

Fig. 7 Spectrum of the non-volatile 4th fraction, from the rotary evaporator fractionation, of a condensate sample (sample #1, Table 1)

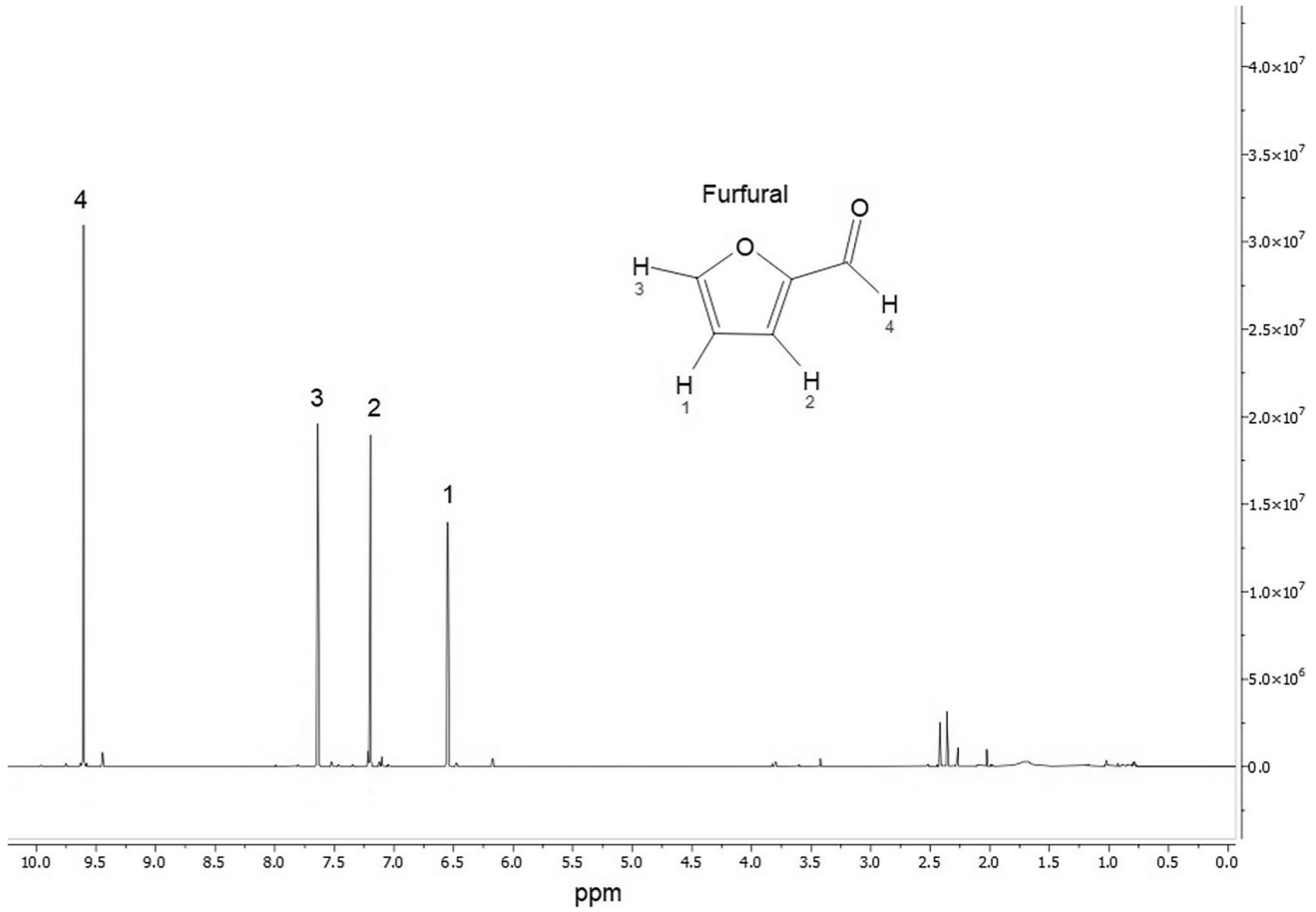

Fig. 8 Proton-NMR spectra of the black liquid, created with a 600-MHz NMR instrument. The most intense peaks assigned showing that it mainly consists of furfural

3.2.4 Fractionation of condensates and GC–MS results

From fractionation with the rotary evaporator, 4 separate fractions were created, where the residual fraction was non-volatile matter and comprised 3.1 wt% of the original condensate sample. In addition to the infrared spectrum given above (Fig. 7), this fraction was analyzed by GC–MS to determine the individual compounds present. The identified components are shown in Table S5 and found to be different terpenoid components from wood extractives.

Condensate samples collected from the outlets of HPC and LPC condenser units will sometimes have a thin yellow layer floating on top. The origin of the organic phase on top of the condensates is thus likely to be terpenoids from the wood biomass, but it also often contains biomass particles from the steam explosion.

3.3 Results from laboratory experiments

The laboratory experiments, listed in Table 5, gave some insights into what may cause the formation of the black particles found in the distillation unit.

Heating the condensate samples to their boiling point had some effects on the visual presentation of the condensate. The color changed from a light transparent yellow to a dark orange and the organic layer on top, consisting of terpenoids, thickened into a more viscous film. There were also some orange deposits staining the glass flask. However, the experiment did not produce any visible solid matter resembling the black particles and the results were therefore inconclusive.

To further investigate whether the black particles could be produced in the lab, two additional experimental variables were investigated. Firstly, a sample of black particles from the ArbaOne plant was added to the condensate sample before heating, to investigate whether we could

Table 5 Results from laboratory experiments to replicate the formation of black particles. The table shows the input factors and the mass difference after the reaction. Furfural is denoted as FF in this table

Experiment/liquid medium		Seeding particles	Added furans	Weight of solids after heating	Mass difference
1.1	Condensate	–	–	0.00	0.00
2.1	Condensate	0.45	–	0.38	−0.07
3.1	Condensate	0.31	4 mL FF	0.41	0.10
2.2	Condensate	0.42	–	0.42	0.00
3.2	Condensate	0.46	4 mL FF	0.55	0.09
1.2	Dest. H_2O	–	–	0.00	0.00
4.1	Condensate	0.44	0.05 g HMF	0.45	0.01
5.1*	Dist. H_2O	–	4 mL FF	0.52	0.52
6.1*	Condensate	–	4 mL FF	0.30	0.30

*Control experiments with only added furfural

induce the growth of the particles with the condensates. Secondly, the furfural concentration was increased by adding a furfural standard (Sigma-Aldrich, 99%) to determine if black particle growth could be induced at any reasonable furfural concentration.

However, heating condensates with the addition of seeding particles had no positive effect on further generation of black particles, but rather a slight decrease in solid mass was found. In spite of this, increasing the concentration of furfural in the sample up to approx. 80 g/L by adding 4 mL of furfural before boiling resulted in a large increase in the solid material of similar character to the original black particles. A control test where furfural was added to both distilled water and a condensate sample and heated to boiling produced dark solid material deposits on the glassware in both instances. The solid residues from the experiments were then analyzed with FTIR (Fig. 9).

The FT-IR spectra in Fig. 10 show the similarities between the black residue created during laboratory experiments with furfural in water/condensate (pink and blue) and the spectra acquired from the black particles (sample #5, Table 1 (orange)).

It is interesting to note how the yield of black residue varies by a large amount in these experiments. While some of the variation can be attributed to difficulty with removing all the solids from the flask without loss, the likely reason for the variation is that the furfural, which was added to the condensate samples in certain experiments, was mixed for an arbitrary amount of time, until it was visually homogeneous in the flask. However, it was observed that in the control experiments with distilled water and furfural, some furfural seemed to fall out of solution with the water and collect on the bottom in small droplets after beginning to heat the mixture. This may be caused by a too short mixing time but shows how furfural in a separate phase in an aqueous medium will increase the yield of solid black residue formed on the hot glass surface and strongly supports the hypothesis of the black particles being formed from polymerization of furfural. Figure 9 shows pictures of the progression of black particle growth from the control experiment, where furfural was added to distilled water.

Fig. 9 Pictures showing the formation of black particles in laboratory experiments (experiment 6.1). Separate droplets of furfural collecting on the bottom (L). Black liquid and particle formation (M) dried particle residue retrieved from the flask (R)

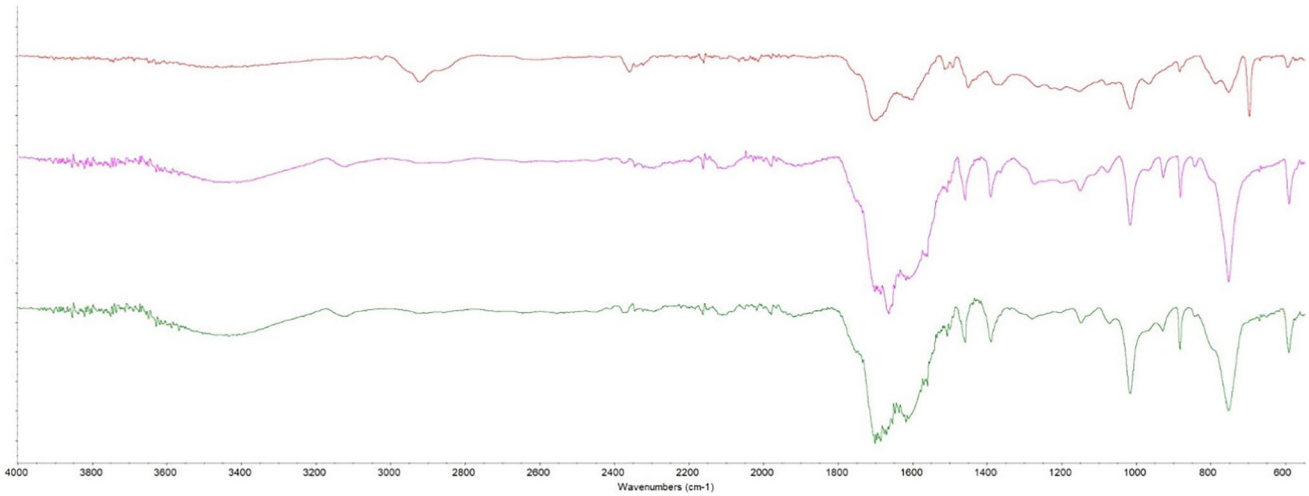

Fig. 10 Figure showing the similarities between residue from black particles from the distillation (top, orange), the control experiment with distilled H_2O (middle, pink), and the unit condensate control experiment (bottom, green)

4 Discussion

The origin of the black particles was hypothesized to be either humins, polymerization of furfural, polymerization of terpenoids, or a co-polymerization of all three compound types. Analysis of the fluid samples (1, 2, 3, and 6) shows the presence of both furfural and terpenoids in the fluid stream, including the existence of a separated furfural phase found in a drainage pipe (sample 6). Furfural is known to readily polymerize to give a black solid [21] while terpenoids are a natural source of wood resins that with time can form insoluble amber.

From the GC–MS analysis of the fractionated condensate and the skimmer tank product (Fig. 7), wood extractives and especially terpenoids are among the most abundant compounds.

In the analysis of the soluble parts of the black particle sample, the components are shown to be dominated by terpenoids, both in direct GC–MS and PY-GC–MS. Most of the identified components contain oxygen, which increases their water solubility and explains why they are not removed in the skimmer tank together with the hydrocarbon terpenoid species. Hence, they are present in the post-skimmer process stream and can be a factor in the formation of black particles downstream in the system.

From the literature definition, humins are defined as by-products from the conversion of cellulose and its derivatives including sugars, HMF, and lactic acid. The humin yield will also generally increase with higher temperatures. In the condensate streams from the Arbaflame process, the concentrations of both HMF and sugars are very low, as they are not volatile and therefore generally stay with the steam-exploded biomass instead of following the steam from the reactor. Additionally, the distillation unit operates at temperatures around 100 °C, which reduces the rates of the reactions that are involved in humin formation. When considering the total throughput of condensate over time, the total amount of sugar and HMF are larger. However, for these to be the primary cause of the black particles, a mechanism is needed where these molecules aggregate on the hot surface of the heat exchanger, which so far have not been shown.

Furfural on the other hand is the most abundant compound in the system, with a propensity for polymerization, and furfural is also the target product for the processing unit. Furfural is formed from hemicellulose sugars at the STEX conditions and is volatile with the steam. It thus follows the steam and is present as a dissolved component in the subsequently condensed aqueous stream. A separate organic phase comprising mostly furfural was also found in the process system, in the form of the dark-colored liquid tapped from a drainage pipe (sample #6). The processes leading to the formation of the separated furfural liquid phase are at present unknown but reflect that the furfural concentration in the aqueous stream must at times be above the solubility limit of 83 g/L. Furfural is thus an accessible source material for polymerization into solid particles. The black color of the particles is consistent with furan-based polymers, as darkening and black precipitates have been widely reported as a problem in furfural production and storage. A suggestion for the structure of the furfural polymer is given in Zeitsch [20] and reproduced here (Fig. 11).

The IR spectra of the particles from the refinery and laboratory experiments, as shown in Figs. 5 and 10, respectively, correspond well with the hypothesis of a furfural origin, as very limited absorption is found in the C–H areas. Terpenoids give strong adsorption around 3000 cm^{-1}, as seen in Fig. 7 from the residual terpenoids from the condensate fractionation. As an example of a terpenoid polymer, reference

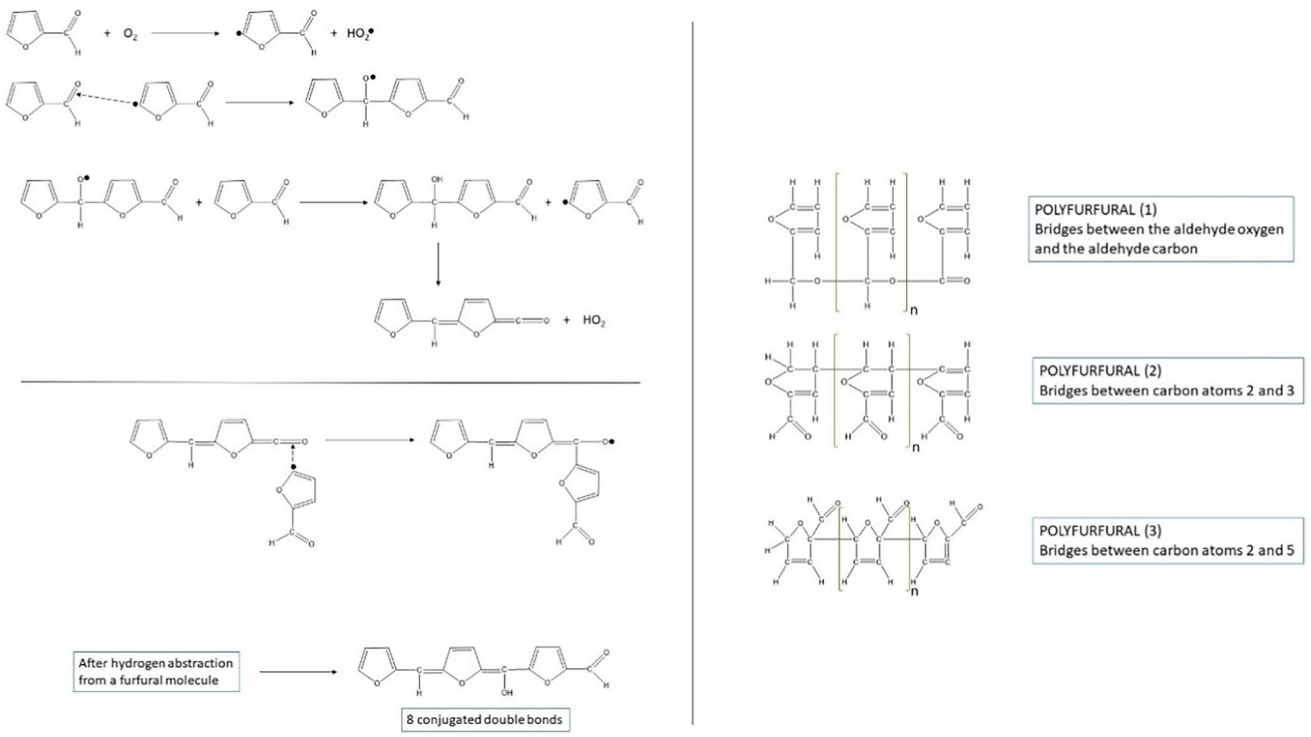

Fig. 11 Suggested reaction mechanism (L) and structures (R) for furfural polymers (adapted from Zeitsch 2000, 30–32 [20])

IR spectra of amber [22] also show strong IR adsorption in the C–H areas, which is not in agreement with the spectra acquired for the black particles in this analysis. Furfural is known to polymerize very efficiently at acidic conditions, and the pH of the condensate is in the area of 2–3 due to the presence of formic and acetic acid produced during hemicellulose degradation at STEX conditions [2]. The presence of catalysts can increase the propensity for polymerization. However, the ash content of the particle is low, and the inorganic constituents are quite limited, which does not support a hypothesis with the presence of active heterogeneous catalysts for this reaction. The polymerization of furfural is expected to be more efficient when the furfural is present as a separate organic phase, as found in sample 6 [23]. Even though no evidence of black particles was found before the distillation unit, there is a possibility that nucleation of the particles starts at an earlier phase, e.g., as humin formation, but that growth occurs at a low rate before they reach the distillation unit. Here temperatures are higher and the presence of heated surfaces where the nucleated particles can attach to and grow on increases. The ultra-filtration unit would however remove humin particles larger than 0.05 µm before reaching the purification unit, suggesting that humin particles, which may be created during the STEX reaction, are not likely to reach the distillation unit.

Compared with humins formed during furfural production from xylose, the black particles have higher oxygen content and a corresponding lower carbon content. The hydrogen content is also very similar but slightly higher in the black particle sample. The theoretical H/C and O/C ratios for polymerized furfural are H/C = 0.8 and O/C = 0.4, according to the polymerization scheme provided in Zeitsch, which is not very different from the measured values for the black particles that average H/C = 0.88 and O/C = 0.26. Aside from these differences, the black particles share many similarities in both properties and apparent structure with both humins [24] and pseudo-lignins, which is another class of solid by-product. Pseudo-lignins are derived from condensation reactions between dehydrated polysaccharides, such as HMF and furfural, that take place during high-severity pretreatment of lignocellulosic biomass in the presence of acids (Fig. 12) [25].

A probable explanation for the terpenoids that have been observed in thermal and solvent extracts can be that they are adsorbed on the surface of the particles. Globules seen on the particle surface in the SEM pictures correspond well with the adsorbed terpenoids. A certain degree of co-polymerization of terpenoids into the primarily furfural-based solids is also possible, which would explain why the measured O/C ratio is lower than the theoretical ratio for a pure furfural polymer. However, the proportion must be quite limited since strong C–H adsorption bands are not seen in the IR spectra. A depiction of the suggested pathway for the formation of black particles from wood can be found in Fig. 13.

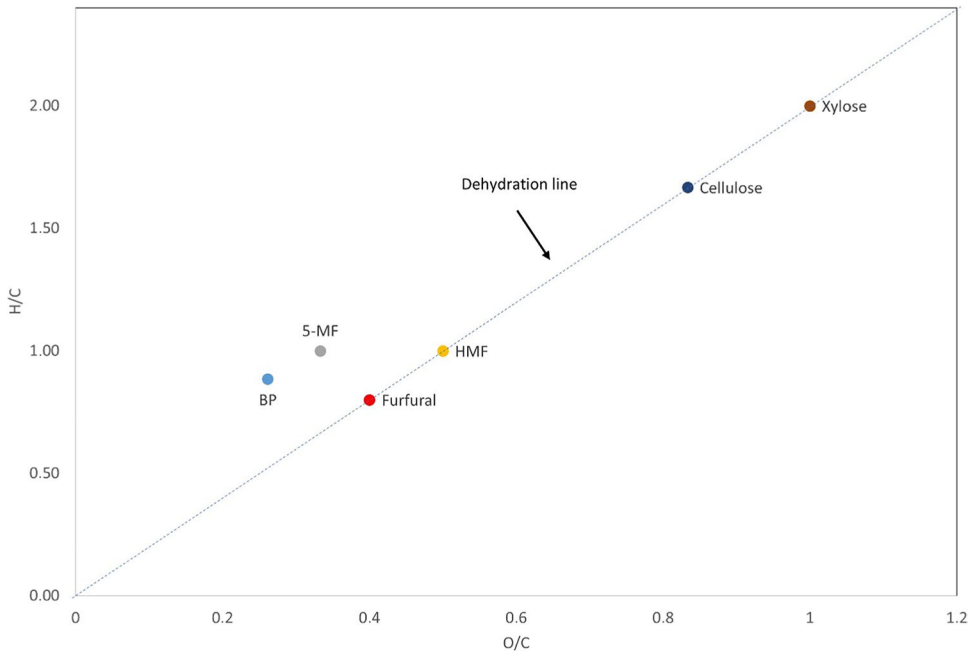

Fig. 12 Van Krevelen diagram comparing the black particles (BP) from furfural production, furans (5-MF, HMF, and furfural) as well as cellulose and xylose (the figure is amended from Wang et al. [6])

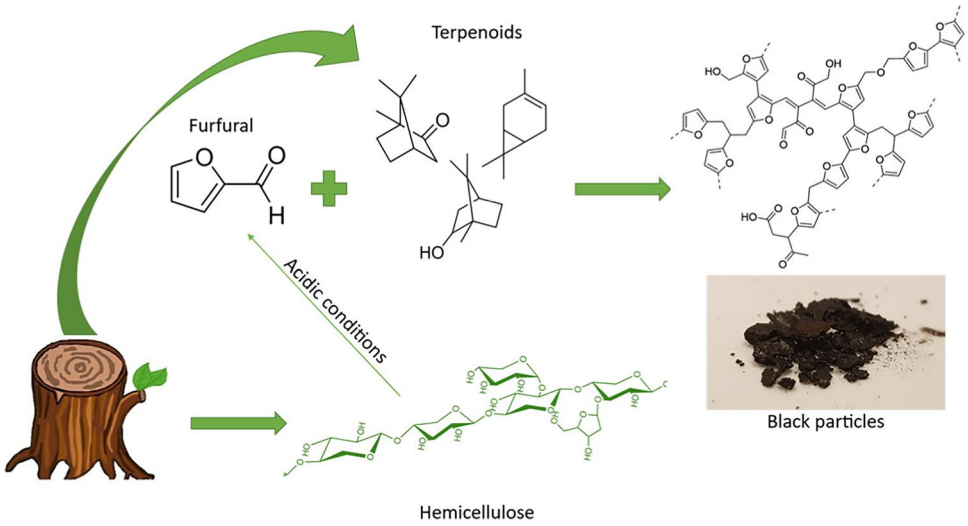

Fig. 13 Schematic overview of the suggested formation pathway for the black particles in the Arbaflame plant

5 Conclusions

Steam explosion of biomass and valorization of chemical by-products is a challenging process where the formation of unwanted solids is almost impossible to avoid. Understanding the conditions that lead to their formation and their chemical structure is therefore necessary for the ability to handle these undesirable solid residues and maintain a fully functional biorefinery.

Analyses performed on black particles found in the distillation unit of the ArbaOne plant, along with analyses of fluids from several different points throughout the side-stream process chain, are presented in this paper and show that these insoluble particles, which have been formed on a heated surface, are of an organic nature and have humin-like characteristics. Our interpretation of the results shows that the black particles recovered from the distillation unit primarily consist of polymerized furfural with a certain amount of adsorbed terpenoids on the particle surface. Some aspects of the reaction mechanism, like the reaction kinetics, have not been investigated in depth in this work and are yet not fully understood. While the analysis of the recovered particles indicates that the structure incorporates organic compounds like terpenoids, laboratory experiments have found that no constituent other

than furfural is necessary for the formation of black solids to happen. A range of other compounds, like other furans and residual sugars, while not as prominent as furfural, can be found in the condensate stream. This permits the possibility that some of these could also be integrated into the complex polymer matrix of the particles.

To prevent the formation of black particles, it is suggested that the concentration of furfural in the condensate be below the saturation point for furfural in water. This also means that distilled furfural without sufficient purity should not be redistilled together with STEX condensate, as this may increase the furfural concentration above the saturation limit, creating a separate furfural phase that can polymerize to black particles. It is also suggested to implement routine cleaning of distillation equipment to limit the negative effects of black particle formation. The use of strong acids is preferred as they have shown to be effective, but solvents or good industrial cleaners may be used as the use of strong acids may not be practical in an industrial setting.

The similarities between the black particles, discussed in this paper, and the other dark solids reported in literature, such as humins and pseudo-lignins, are presumably not arbitrary. The resemblance emerges because of the requirement for very similar substrates and reaction conditions. How the black particles produced at the ArbaOne plant, during distillation of furfural, should be characterized in relation to humins, defined by their generation from catalytic conversion of cellulose and its derivatives, and pseudo-lignins, which arise from condensation reactions during high-severity, acidic pretreatment, is not within the scope of this paper. Moving forward, the focus should be on investigating the reaction kinetics of the furfural polymerization, to better understand the conditions necessary to trigger these polymerization reactions.

Supplementary information The online version contains supplementary material available at https://doi.org/10.1007/s13399-022-03593-9.

Acknowledgements The authors would like to acknowledge Siv Dundas for assisting with the ICP-MS analysis, Irene Heggestad at the ELMilab for assistance with the SEM imaging, Inger J. Fjellanger for assistance with the elemental analysis, and Kenneth Aasarød from RISE PFI for assistance with the TGA-FTIR analysis. We would also like to thank Stine Johansen at the ArbaOne plant for assistance with on-site work and Joakim L. Molnes for his graphical contribution and help with text revision. This work was partly supported by the Bergen Research Foundation (BFS-NMR-1), Sparebankstiftinga Sogn og Fjordane (509-42/16), and the Research Council of Norway through the Norwegian NMR Platform, NNP (226244/F50).

Author contribution The experimental work was carried out by Dag Helge Hermundsgård, Solmaz Ghoreishi, and Mihaela Tanase-Opedal. Writing was carried out by Tanja Barth and Dag Helge Hermundsgård. Rune Brusletto developed the ArbaOne concept and implemented it in the production unit. Solmaz Ghoreishi and Mihaela Tanase-Opedal have also contributed with the text revision.

Funding Open access funding provided by University of Bergen (incl Haukeland University Hospital) This work received funding from Arbaflame AS through the Research Council of Norway under grant agreement No 309970 and Ph.D. project No 321268.

Declarations

Conflict of interest The authors declare no competing interests.

References

1. ArbaOne (n.d) About Arbaflame. Accessed 10 Aug 2022.https://www.arbaflame.no/about-arbaflame
2. Ghoreishi S et al (2022) Identification and quantification of valuable platform chemicals in aqueous product streams from a preliminary study of large pilot-scale steam explosion of woody biomass using quantitative nuclear magnetic resonance spectroscopy. Biomass Convers Biorefinery (2022) 1–19. https://doi.org/10.1007/s13399-022-02712-w
3. Sjöström E (1993) Wood chemistry: fundamentals and applications 2nd edt. Academic Press, San Diego
4. de Jong Ed et al (2022) "The road to bring FDCA and PEF to the market". Polymers 14(5):943. https://doi.org/10.3390/polym14050943
5. van Zandvoort et al (2013) Formation, molecular structure and morphology of humins in biomass conversion: influence of feedstock and processing conditions" ChemSusChem 6:1745-1758.https://doi.org/10.1002/cssc.201300332
6. WangLinZhaoChenZhou SHYJJ (2016) Structural characterization and pyrolysis behavior of humin by-products from the acid-catalyzed conversion of C6 and C5 carbohydrates. J Anal Appl Pyrol 118:259–266. https://doi.org/10.1016/j.jaap.2016.02.009
7. PatilHeltzelLund SKRJCRF (2012) Comparison of structural features of humins formed catalytically from glucose, fructose, and 5-hydroxymethylfurfuraldehyde. Energy Fuels 26(8):5281–5293. https://doi.org/10.1021/ef3007454
8. Tosi et al (2018) Auto-crosslinked rigid foams derived from biorefinery byproducts". ChemSusChem 11(16):2797-2809.https://doi.org/10.1002/cssc.201800778
9. GirisutaJanssenHeeres BLPBMHJ (2006) A kinetic study on the decomposition of 5-hydroxymethylfurfural into levulinic acid. Green Chem 8:701–709. https://doi.org/10.1039/B518176C
10. GirisutaJanssenHeeres BLPBMHJ (2007) Kinetic study on the acid-catalyzed hydrolysis of cellulose to levulinic acid. Ind Eng Chem Res 46:1696–1708. https://doi.org/10.1021/ie061186z
11. Girisuta B et al (2008) Experimental and kinetic modelling studies on the acid-catalysed hydrolysis of the water hyacinth plant

to levulinic acid. Biores Technol 99:8367–8375. https://doi.org/10.1016/j.biortech.2008.02.045
12. MerkleinFongDeng KSSY (2016) Biomass utilization in biotechnology for biofuel production and optimization. Elsevier, Amsterdam, pp 291–324
13. Brusletto R, Kleinert M (2018) Method of producing carbon enriched biomass material (Patent). Patent number: US 10,119,088 B2. https://patents.google.com/patent/US10119088B2/en
14. Brusletto R, Plückhahn W (2019) Method and apparatus for preparing fuel from biomass (Patent). Patent number: US 10,287,525 B2. https://patents.google.com/patent/US20160002555A1
15. Tosi P (2019) Building new tomorrows for humins as biorefinery by product through the design of porous materials and applications, Chapter 2: Humins - A review, Chemical engineering. COMUE Université Côte d'Azur (2015–2019) pp 5–55
16. GirisutaJanssenHeeres BLPBMHJ (2006) A kinetic study on the conversion of glucose to levulinic acid. Chem Eng Res Design 84(5):339–349. https://doi.org/10.1205/cherd05038
17. BaughMcCarty KDPL (1988) Thermochemical pretreatment of lignocellulose to enhance methane fermentation: I. Monosaccharide and furfurals hydrothermal decomposition and product formation rates. Biotechnol Bioeng 31:50–61. https://doi.org/10.1002/bit.260310109
18. Luijkx GCA, van Rantwijk F, van Bekkum H (1993). "Hydrothermal formation of 1,2,4-benzenetriol from 5-hydroxymethyl-2-furaldehyde and d-fructose". Carbohydr Res 242:131–139.https://doi.org/10.1016/0008-6215(93)80027-C
19. Flores J et al (2020) Thermal degradation and FT-IR analysis on the pyrolysis of pinus pseudostrobus, Pinus leiophylla and Pinus montezumae as forest waste in Western Mexico. Energies 2020(13):969. https://doi.org/10.3390/en13040969
20. Lamminpää K, Ahola J, Tanskanen J (2014) Kinetics of furfural destruction in a formic acid medium. RSC Adv 4:60243–60248. https://doi.org/10.1039/C4RA09276G
21. Zeitsch KJ (2000) The chemistry and technology of furfural and its many by-products. Elsevier Science, Amsterdam
22. Villanueva-García M, Martínez-Richa A, Robles J (2005) Assignment of vibrational spectra of labdatriene derivatives and ambers: a combined experimental and density functional theoretical study. Arkivoc 2005(6):449–458. https://doi.org/10.3998/ark.5550190.0006.639
23. GhattaZhouCasaranoWilton-ElyHallett AAXGJDETJP (2021) Characterization and valorisation of humins produced by HMF degradation in ionic liquids: a valuable carbonaceous material for antimony removal. ACS Sustain Chem Eng 9:2212–2223. https://doi.org/10.1021/acssuschemeng.0c07963
24. Liu S et al (2022) Advances in understanding the humins: formation, prevention and application". Appl Energy Combust Sci 10:100062. https://doi.org/10.1016/j.jaecs.2022.100062
25. ShindeMengKumarRagauskas SXRA (2018) Recent advances in understanding the pseudo-lignin formation in a lignocellulosic biorefinery. Green Chem 20:2192–2205. https://doi.org/10.1039/C8GC00353J